Evidence for $B^- \to D^{**0}\tau^-\bar{\nu}_\tau$ Decays

R. Aaij *et al.*[*]
(LHCb Collaboration)

(Received 31 January 2025; accepted 27 May 2025; published 8 July 2025)

The first evidence for the decay $B^- \to D^{**0}\tau^-\bar{\nu}_\tau$ is obtained using proton-proton collision data collected by the LHCb experiment, corresponding to an integrated luminosity of 9 fb^{-1}, at centre-of-mass energies of 7, 8, and 13 TeV. Here, the D^{**0} meson represents any of the three excited charm mesons $D_1(2420)^0$, $D_2^*(2460)^0$, and $D_1'(2400)^0$. The $B^- \to D^{**0}\tau^-\bar{\nu}_\tau$ signal is measured with a significance of 3.5σ, including systematic uncertainties. The combined branching fraction $\mathcal{B}(B^- \to D_{1,2}^{**0}\tau^-\bar{\nu}_\tau) \times \mathcal{B}(D_{1,2}^{**0} \to D^{*+}\pi^-)$, where $D_{1,2}^{**0}$ denotes both $D_1(2420)^0$ and $D_2^*(2460)^0$ contributions, is measured to be $[0.051 \pm 0.013(\text{stat}) \pm 0.006(\text{syst}) \pm 0.009(\text{ext})]\%$, where the last uncertainty reflects that of the branching fraction of the normalization channel $B^- \to D_{1,2}^{**0}D_s^{-(*)}$. The ratio between the tauonic and muonic semileptonic B decays, with the latter taken from world average values, is also determined and found to be $\mathcal{R}(D_{1,2}^{**0}) = 0.13 \pm 0.03(\text{stat}) \pm 0.01(\text{syst}) \pm 0.02(\text{ext})$.

DOI: 10.1103/rj9h-n4w1

Lepton flavor universality (LFU) is one of the pillars of the standard model (SM) of particle physics. It postulates that the three charged leptons have exactly the same properties and couplings, except for their masses. However, LFU is often violated in models beyond the SM [1,2]. Experimentally [3–12], evidence of LFU violation is found in semileptonic B decays, where the ratio of branching fractions $\mathcal{R}(D^{(*)})$, defined as $\mathcal{B}(B \to D^{(*)}\tau^-\bar{\nu}_\tau)/\mathcal{B}(B \to D^{(*)}\mu^-\bar{\nu}_\mu)$, exceeds its SM prediction by 3.3 standard deviations (σ) [13]. This long-standing discrepancy calls for more investigations of potential systematic effects. One of the largest systematic uncertainties common to all $\mathcal{R}(D^{(*)})$ measurements is the limited knowledge of the $D^{*+}\tau^-\bar{\nu}_\tau$ contamination by $B \to D^{**}\tau^-\bar{\nu}_\tau$ decays, where D^{**} mesons decay to a state containing a D^{*+} meson [13]. Hereafter, the D^{**} symbol designates all excited $c\bar{u}$ and $c\bar{d}$ mesons more massive than the $D^*(2010)$ state. The four lightest states are $D_0^*(2300)$, $D_1(2420)$, $D_1'(2400)$, and $D_2^*(2460)$ with masses 2343, 2422, 2412, and 2461 MeV/c^2, respectively [14]. The last three mesons decay significantly into $D^*\,\pi$, while the first one decays only to $D\pi$. The $D_1(2420)$ and $D_2^*(2460)$ states are narrow with widths of 31 and 47 MeV/c^2 [14], while the other two are very wide with widths in the range 200–300 MeV/c^2. Theoretical predictions regarding the branching fractions of the D^{**0} mesons to the $D^{*+}\pi^-$ final state can be found in Ref. [15].

The goal of this analysis is to search for the $B^- \to D^{**0}\tau^-\bar{\nu}_\tau$ decays, and measure the branching fraction of the $B^- \to D_{1,2}^{**0}\tau^-\bar{\nu}_\tau$ decay, where $D_{1,2}^{**0}$ represents the combined contributions from the $D_1(2420)^0$ and $D_2^*(2460)^0$ mesons. The $D_{1,2}^{**0}$ mesons are reconstructed from the $K^-\pi^-\pi^+\pi^+$ final state using the $D_{1,2}^{**0} \to D^{*+}\pi^-$, $D^{*+} \to D^0\pi^+$, $D^0 \to K^-\pi^+$ decay chain. (The inclusion of charge-conjugate processes is implied throughout, unless otherwise stated.) The τ^- lepton is reconstructed using the $\tau^- \to \pi^-\pi^+\pi^-(\pi^0)\nu_\tau$ decay, where the π^0 meson is not reconstructed. The decay $B^- \to D_{1,2}^{**0}D_s^{-(*)}$ is used as normalization channel for the branching fraction measurement. Its branching fraction is extracted from the recent analysis by the LHCb Collaboration [16]. The normalization channel is reconstructed using the $D_s^- \to \pi^-\pi^+\pi^-$ decay that features the same vertex topology and visible final state of the signal decay. Many systematic uncertainties are in common between the two channels and cancel out in the measurement of the ratio of branching fractions. Using the known $\mathcal{B}(B \to D_{1,2}^{**0}\mu^-\bar{\nu}_\mu)$ value [14], the ratio $\mathcal{R}(D_{1,2}^{**0}) \equiv \mathcal{B}(B \to D_{1,2}^{**0}\tau^-\bar{\nu}_\tau)/\mathcal{B}(B \to D_{1,2}^{**0}\mu^-\bar{\nu}_\mu)$ can also be determined and compared to the assumptions used in the $\mathcal{R}(D^{(*)})$ measurements [3–12].

This analysis uses a data sample of proton-proton (pp) collisions collected with the LHCb detector, at center-of-mass energies of 7, 8, and 13 TeV, corresponding to an integrated luminosity of 9 fb^{-1}. The LHCb detector is a single-arm forward spectrometer covering the pseudorapidity range

[*]Full author list given at the end of the Letter.

$2 < \eta < 5$, described in detail in Refs. [17,18]. The detector includes a high-precision tracking system consisting of a silicon-strip vertex detector surrounding the pp interaction region [19], and large-area silicon-strip detectors located upstream and downstream of the 4 T m dipole magnet. The minimum distance of a track to a primary pp collision vertex (PV), the impact parameter (IP), is measured with a resolution of $(15 + 29/p_{\mathrm{T}})$ μm, where p_{T} is the component of the momentum transverse to the beam direction, in GeV/c. The online event selection is performed by a trigger system [20], which consists of a hardware stage based on information from the calorimeter and muon systems, followed by a software stage that performs a full event reconstruction. Events are selected at the hardware stage if the particles forming the signal candidate satisfy a requirement on the energy deposited in the calorimeters or if any other particle passes any trigger requirement. The software trigger requires a two-, three-, or four-track secondary vertex with significant displacement from any PV and consistent with the decay of a b hadron, or a three-track vertex with a significant displacement from any PV and consistent with the decay of a D^* meson. A multivariate algorithm [21,22] is used for the identification of secondary vertices. In the simulation, pp collisions are generated using PYTHIA 8 [23] with a specific LHCb configuration [24]. Decays of hadronic particles are described by EvtGen [25], in which final-state radiation is generated using PHOTOS [26]. The Tauola package [27] is used to simulate the decays of the τ^- lepton into $\pi^-\pi^-\pi^+\nu_\tau$ and $\pi^-\pi^-\pi^+\pi^0\nu_\tau$ final states, according to the resonance chiral Lagrangian model [28] with a tuning based on the results from the *BABAR* Collaboration [29]. The interaction of the generated particles with the detector, and its response, is implemented using the Geant4 toolkit [30] as described in Ref. [31].

This analysis follows the same selection regarding the reconstruction of D^{*+} and τ^- candidates as the $\mathcal{R}(D^*)$ measurement [9]. The presence of exactly one extra pion track, compatible with originating from the B^- vertex is also required. Samples of right-sign (RS) or wrong-sign (WS) D^{**} candidates are then formed by combining selected D^{*+} candidates with a pion track compatible with originating from the B^- vertex, having opposite or same charge, respectively. The B^- candidate is reconstructed from the combination of the D^{**0} and τ^- candidates. The pion and the D^{*+} decay products are required to form a good-quality vertex. The D^0 and D^{*+} candidates are required to have a mass close to their known values [14], and mass sidebands are used to subtract the background. As in previous analyses [8,9,32], a stringent requirement is applied to the displacement along the beam axis between the τ^- and B^- vertices, which must exceed 4 times the associated uncertainty. This selection is highly effective in suppressing the so-called *prompt* background, due to $B \to D^{**0}\pi^-\pi^-\pi^+X$ combinations, where the pion triplet is produced at the B decay vertex and X denotes additional undetected particles (including zero if specified in parentheses).

A boosted decision tree (BDT) [21] classifier is trained to reject the background due to $B \to D^{*+}D_s^-(X)$ events, where a π^- meson from a five-prong D_s^- decay is combined with the D^{*+} to form the D^{**0} candidate. The classifier exploits the different vertex topology between this background and the signal, and is trained using simulated samples of the two decays. This classifier is also efficient in reducing the prompt background, where the π^- meson used to form the D^{**0} candidate and the pion triplet are produced at the same vertex. A second BDT classifier is used to reject remaining fake D^{**} candidates and is trained using simulated $B^- \to D_1(2420)^0\tau^-\bar{\nu}_\tau$ events as signal and the WS data as background. A further BDT classifier, referred to as BDT-antiD_s, is optimized to suppress the main background arising from D_s^- decays to three pions which mimics τ^- decays. It uses the same inputs as for $\mathcal{R}(D^*)$ measurement [9]. This classifier leverages the distinct decay dynamics of the signal τ^- decays and the D_s^- decays, and is used in the signal extraction procedure.

The D^{**0} candidates mass distribution after the final selection except the BDT-antiD_s requirement and the upper limit of 1600 MeV/c^2 on the $\pi^-\pi^+\pi^-$ mass is shown in Fig. 1. To improve the resolution, the mass is calculated using the known D^{*+} mass [14], $M_{D^{*+}}$, and the difference between the masses of the D^{**0} and D^{*+} candidates, $\Delta m \equiv m(D^{*+}\pi^-) - m(D^{*+})$, as $m(D^{*+}\pi^-) \equiv \Delta m + M_{D^{*+}}$. An unbinned maximum-likelihood fit to the mass distribution is performed using two relativistic Breit-Wigner functions to describe the signal and one exponential function for the background. The yields of $D_1(2420)^0$ and $D_2^*(2460)^0$ contributions are found to be 2456 ± 75 and 633 ± 69, respectively. These results allow to determine the typical size and composition

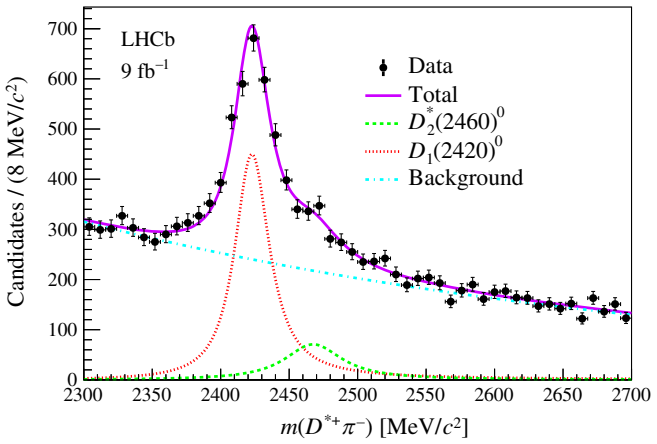

FIG. 1. Distribution of the $D^{*+}\pi^-$ mass for all selected $D^{**0}\pi^-\pi^-\pi^+$ candidates in the full dataset, with the result of the fit also shown A potential $D_1'(2400)^0$ component can not be distinguished from the background.

TABLE I. List of the various background categories. The first, second and third columns indicate the decay chain producing each background, the control sample dedicated to its study, and an estimate of its relative contribution in the selected sample, reflected by the number of stars, respectively.

Background source	Control sample	Size
Fake D^{**0}		
Fake D^0 or fake D^{*+}	D^0 and D^{*+} sidebands	*
Genuine D^{*+}; fake D^{**0}	WS sample	***
	$B \to D^{*+}D^{*-}(X)$	*
	$B \to D^{*+}(DK)^-(X)$	**
Genuine D^{**0}		
$B \to D^{**0}\pi^-\pi^-\pi^+X$	$B^- \to D^{**0}\pi^-\pi^-\pi^+$	*
$B^- \to D^{**0}D_s^-(X)$	$B^- \to D^{*+}D_s^-(\to \pi^-\pi^-\pi^+)(X)$	***
$B^- \to D^{**0}(DK)^-$	$B \to D^{*+}D^0(\to K^-\pi^+\pi^+\pi^-)(X)$	Negligible

in terms of $D_1(2420)^0$ to $D_2^*(2460)^0$ ratio of the initial D^{**0} meson sample, but are not explicitly used in the following.

Various background sources contribute to the $B^- \to D^{**0}\tau^-\bar{\nu}_\tau$ selected sample. Their yields and distributions are determined using control data samples. Table I summarizes the main background contributions and the corresponding control samples. Fake D^0 or D^{*+} candidates are removed using the sideband subtraction method. Fake D^{**0} mesons can be formed combining a genuine D^{*+} meson with a random pion. This background source is studied using the WS sample, leveraging the fact that random pions are equally likely to carry either charge. Candidates from $B \to D^{*+}D_s^-(X)$ and $D_s^- \to \pi^-\pi^-\pi^-\pi^+\pi^+$ decays and random $D^{*+}\pi^-$ combinations fall into this category. Possible sources producing only WS combinations are investigated; the only significant one stems from the wrong reconstruction of the slow pion from the $D^{*-} \to \bar{D}^0\pi^-$ decay into two almost identical tracks, one being used to form a D^{*+} candidate and the other to form a WS D^{**0} candidate. Such cases are removed with a requirement on a dedicated multivariate classifier. Additionally, fake D^{**0} mesons can arise from $B \to D^{*+}D^{*-}(X)$ decays, where the slow pion is combined with the genuine D^{*+} meson to form the D^{**0} candidate. They can also originate from $B \to D^{*+}(DK)^-(X)$ decays, where the kaon is misidentified as a pion and is combined with the genuine D^{*+} meson. The latter two contributions are not included in the WS sample and must be added separately. These combined contributions represent a good description of the background as indicated from the simulated sample of inclusive b-hadron decays to final states containing $D^{*+}\pi^-\pi^+\pi^-$ that mimics the data as closely as possible as shown in Fig. 5.

The remaining background candidates consist of a genuine D^{**0} candidate associated with a fake τ^- candidate. The largest source of this background is the *prompt* $B \to D^{**0}\pi^-\pi^-\pi^+X$ decay. However, its contribution is suppressed by a factor 10^{-3} due to the detachment requirement on the B^- and τ^- vertices, resulting in an estimated yield of 32 ± 15. This background can be studied using a control sample obtained by removing the detachment selection requirement and analyzing the exclusive decay $B \to D^{**0}\pi^-\pi^-\pi^+$. The remaining candidates arise mostly from $B^- \to D^{**0}D_s^-(X)$ decays, with $D_s^- \to \pi^-\pi^+\pi^-(X)$ decays. The refined model used to describe the inclusive D_s^- meson decays to three and five pions is based on recent measurements perfomed by the BESIII Collaboration [33–40] and is identical to the one in the $\mathcal{R}(D^*)$ analysis [9], as well as the weighting procedure described therein. The corresponding control sample is formed by selecting the exclusive decay $B^- \to D^{**0}\pi^-\pi^-\pi^+$ where the $\pi^-\pi^+\pi^-$ mass is required to be within ± 30 MeV/c^2 of the known D_s^- mass [14]. A data-driven method is used to estimate the relative proportions of D_s^-, D_s^{*-}, and D_s^{**-} mesons associated with a D^{**0} candidate in B^- decays, which are an important input for a correct background description but are poorly known. The method uses a data sample obtained without the BDT-antiD_s^+ selection, but requiring the D_s^- fully reconstructed in the $\pi^+\pi^-\pi^-$ final state. Figure 2 shows the $D^{*+}\pi^-\pi^-\pi^-\pi^+$ mass distribution of the selected candidates. One can identify three regions from left to right: the $B^- \to D^{**0}D_s^{**-}$, $B^- \to D^{**0}D_s^{*-}$, $B^- \to D^{**0}D_s^-$ domains defined with $D^{**0}3\pi$ mass in the ranges below 5000 MeV/c^2, 5000–5200 MeV/c^2, and 5250–5350 MeV/c^2, respectively. Together with the results obtained in Ref. [16] using the $B^- \to D^{*+}D_s^-\pi^-$ and $D_s^- \to K^-K^+\pi^-$ decay chains, this information is used to constrain the yields of the various D_s^- contributions. Furthermore, the yields of $B^- \to D^{**0}D_s^{*-}$ and $B^- \to D^{**0}D_s^-$ are determined to provide the normalization for the branching fraction measurement. The fraction of $D_{1,2}^{**0}$ candidates in these yields are derived from the fit fraction of Ref. [16].

Background due to $B^- \to D^{**0}(DK)^-$ decays, where the notation $(DK)^-$ represents all combinations of a charmed meson and a kaon with a negative total charge, could also contribute, but this source is expected to be highly suppressed due to the limited phase space available.

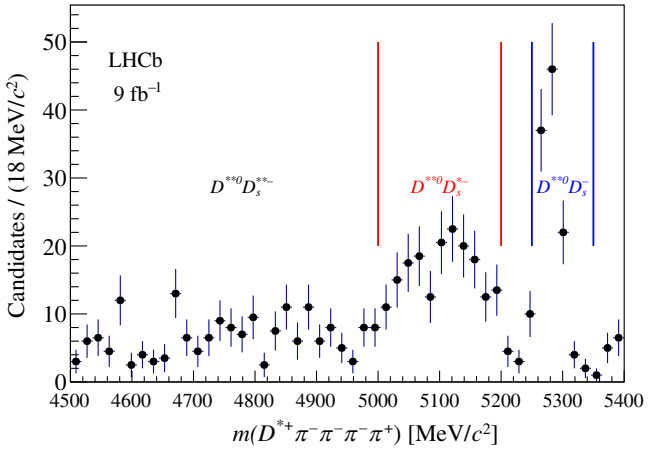

FIG. 2. Distribution of the $D^{*+}\pi^-\pi^-\pi^-\pi^+$ mass for candidates with $\pi^-\pi^+\pi^-$ mass consistent with the D_s^- mass. Background is subtracted using candidates in the D_s^- mass sidebands. Three regions corresponding from left to right to $B^- \to D^{**0}D_s^{**-}$, $B^- \to D^{**0}D_s^{*-}$, and $B^- \to D^{**0}D_s^-$ are indicated by the vertical lines.

Its contribution is studied using control samples obtained requiring a D^{*+} candidate and either a $\bar{D}^0 \to K^+\pi^-\pi^-\pi^+$ or a $D^- \to K^+\pi^-\pi^-$ candidate, where the K^+ track is consistent with originating from the $\pi^-\pi^+\pi^-$ vertex. The first sample, consisting of 42 ± 15 $B^- \to D^{**0}\bar{D}^0K^-$ decays where the K^- track is not reconstructed, as can be seen in Fig. 4, corresponds to an expected yield of 5 ± 3, given the relative efficiencies between the control and signal sample [9]. The second sample leads to a similar contribution. As a result, the background including a genuine D^{**0} is assumed to consist only of the *prompt* $B \to D^{**0}\pi^-\pi^-\pi^-X$ and the $B^- \to D^{**0}D_s^-(X)$ contributions.

As in Ref. [9], the determination of the signal yield is performed using a three-dimensional binned maximum-likelihood fit to the output of the BDT-antiD_s classifier, the squared mass of the $\tau^-\bar{\nu}_\tau$ system, q^2, and the mass difference Δm. This latter variable is used to differentiate between $B^- \to D_{1,2}^{**0}\tau^-\bar{\nu}_\tau$ and $B^- \to D_1'(2400)^0\tau^-\bar{\nu}_\tau$ signals while the BDT-antiD_s classifier separates background contributions such as $B^- \to D^{**0}D_s^-(X)$ decays from signal decays. Given the limited size of the data sample and to reduce the number of empty bins, the fit uses 8 bins for Δm, 5 for the BDT-antiD_s output, and 3 for q^2. The q^2 variable is computed exactly as in Ref. [9]. Taking into account the extra pion from the D^{**0} decay leads to the same signal yield within 2%, taken into account in the systematic uncertainty assigned to the fitting procedure. Simulation and control samples are used to determine the templates that contribute to the final fit: the $B^- \to D^{**0}\tau^-\bar{\nu}_\tau$, $B^- \to D^{**0}D_s^-(X)$ and *prompt* $B \to D^{**0}\pi^-\pi^+\pi^-X$ simulated samples, the WS control sample, together with two simulated samples of $B \to D^{*+}D^{*-}(X)$ and $B \to D^{*+}(DK)^-(X)$ decays. Seven $B^0 \to D^{*+}D_s^-(X)$ templates are used in total, of which six account for the combinations of D_s^- and D_s^{*-} mesons with each of the three D^{**0} mesons, and one includes all D_s^{**-} contributions. The signal templates are computed for each of the three $D_1(2420)^0$, $D_2^*(2460)^0$, and $D_1'(2400)^0$ states. Given the small mass difference between the $D_1(2420)^0$ and the $D_2^*(2460)^0$ states, a common template is used for the sum of the two signal components. Their relative contribution is obtained from their predicted production ratio and branching fractions to $D^{*+}\pi^-$ final states [15]. The relative contribution of $D_1'(2400)^0$ with respect to $D_{1,2}^{**0}$ is constrained to the theoretical prediction of 0.4 ± 0.5 [41,42]. The yields of five components [signal, $B^- \to D_1(2420)^0D_s^{*-}$, $B \to D^{*+}D^{*-}(X)$, $B \to D^{*+}DK(X)$, and the WS templates] are free to float in the fit, while the remaining yields are constrained to the corresponding estimated values. Figure 3 shows the distributions of the three observables, together with the fit projections. The χ^2 per degree of freedom is 0.89, with 115 degrees of freedom, demonstrating a good understanding of the various backgrounds. The $B^- \to D_{1,2}^{**0}\tau^-\bar{\nu}_\tau$ and $B^- \to D^{**0}\tau^-\bar{\nu}_\tau$ decays yields are found to be 123 ± 23 and 220 ± 34, respectively. The quoted uncertainty is statistical, and includes the effects of the Gaussian constraints used in the fit.

The significance of the decay $B^- \to D^{**0}\tau^-\bar{\nu}_\tau$, including a possible contribution from $D_1'(2400)^0\tau^-\bar{\nu}_\tau$, is determined to be 3.5σ, including the systematic uncertainties related to the signal yield determination discussed below. The significance level is obtained comparing the results of a fit to the data allowing the contributions from $B^- \to D^{**0}D_s^{**-}$ and the relative rates of $D_1(2420)^0$ and $D_2^*(2460)^0$ to vary freely, against those of a fit including only background.

The signal yield is compared to the normalization channel yield to derive the branching fraction ratio $\kappa_{D_{1,2}^{**0}}$, through the relation

$$\kappa_{D_{1,2}^{**0}} \equiv \frac{\mathcal{B}(B^- \to D_{1,2}^{**0}\tau^-\bar{\nu}_\tau)}{\mathcal{B}(B^- \to D_{1,2}^{**0}D_s^{(*)-})} = \frac{N_{\text{signal}}}{N_{\text{norm}}} \times \frac{\mathcal{B}(D_s^- \to \pi^-\pi^-\pi^+)}{\mathcal{B}(\tau^- \to \pi^-\pi^-\pi^+(X)) \times \epsilon_R}, \quad (1)$$

where N_{signal} is the signal yield, N_{norm} denotes the yield of the normalization channel, and ϵ_R is the ratio of selection efficiencies between the two channels.

Various effects are studied to assess the systematic uncertainty on the branching fraction ratio $\kappa_{D_{1,2}^{**0}}$. In order to check the fit stability and potential bias, the same fit procedure is performed on selected candidates from the simulated sample containing inclusive b-hadron decays to final states containing $D^*\pi^-\pi^+\pi^-$, and with a signal-to-background ratio similar to that observed in data, and with

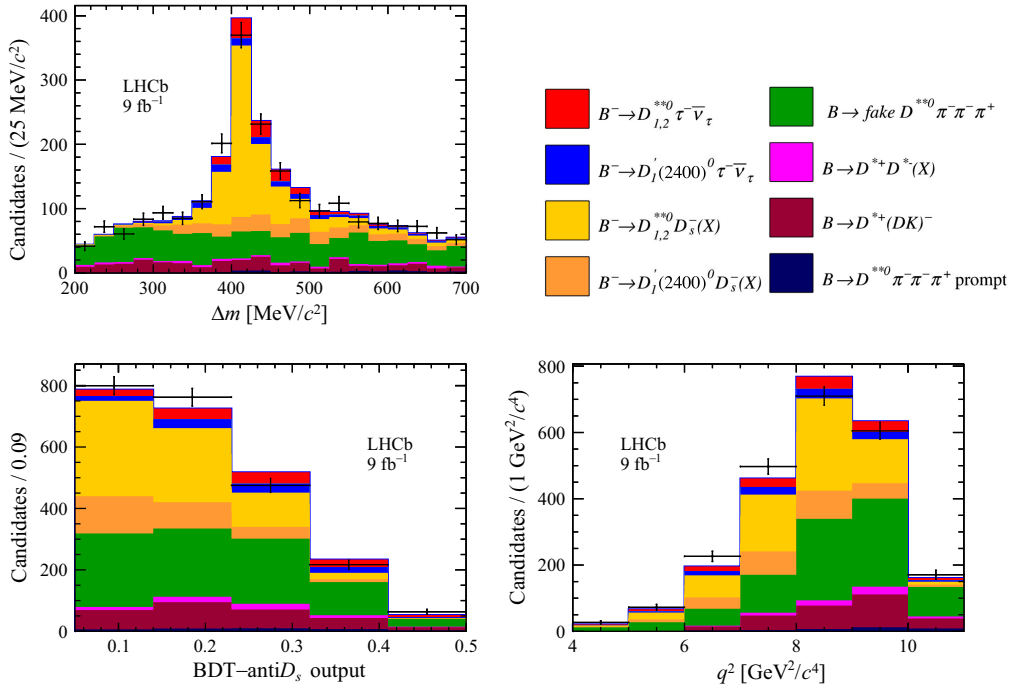

FIG. 3. Top: distribution of the mass difference between the D^{**0} mass and the D^{*+} mass, bottom left: BDT-antiD_s output distribution, and bottom right: distribution of the $\tau^-\bar{\nu}_\tau$ invariant mass squared, q^2, for all candidates fulfilling the final D^{**} selection. The fake D^{**0} component is constructed with the WS data sample.

an equivalent luminosity 10 times larger. The $D^{**0}_{1,2}$ signal yield is found to be compatible within $\pm 1\sigma$ with the true signal yield in the simulated sample. Additional studies are performed with progressively decreasing signal yields. In all cases, the extracted signal yields are found to be in good agreement with the number of signal candidates present in the simulated samples. In an extreme scenario where no signal candidates are simulated, the fit returned a result of 35 ± 80, which is consistent with zero, corresponding to a potential yield in the data of 4 ± 25 events. In the simulation, the three $B^- \to D^{**0}\tau^-\bar{\nu}_\tau$ decays are generated using the Isgur-Scora-Grinstein-Wise (ISGW2) model [43]. More recent models better describe these semileptonic decays: Leibovich-Ligeti-Stewart-Wise (LLSW) [44] and Bernlochner-Ligeti-Robinson (BLR) [41]. Alternative templates are obtained for the main $B^- \to D_1(2420)^0\tau^-\bar{\nu}_\tau$ contribution by using the HAMMER package [45] to weight events according to these two models. The q^2 distributions for each model are shown in Fig. 6. The yields obtained with the LLSW and BLR models are found to be compatible with the baseline result using the ISGW2 model, and the 3.7% relative difference found is assigned as the systematic uncertainty due to the limited knowledge of the form-factor distributions. The fit assumes a fixed ratio between the $D_1(2420)^0$ and $D_2^*(2460)^0$ signal contributions: a systematic uncertainty of 4.4% is assigned by varying their ratio from 0 to 1. The fit χ^2 increases for large $D_2^*(2460)^0$ contributions, a pure $D_2^*(2460)^0$ component is excluded at the level of 2.7σ, and a 50% $D_2^*(2460)^0$ component is disfavored at the 2σ level.

The systematic uncertainty associated with the finite size of the simulated samples leads to an uncertainty of 4.3% for the efficiency computation and 4.1% for the template shapes determined using the bootstrap method [46], as in Ref. [9]. The effect of changing fit observables, replacing the q^2 variable by the D^* helicity angle [47], and changing the binning schemes with half or twice the number of bins, results in a systematic uncertainty of 5.0%, corresponding to half the maximum deviation from the baseline result. The systematic uncertainty associated with the $B^- \to D^{**0}(DK)^-$ background contamination is estimated to be 3.6%, under the assumption that half of the estimated yield consists of signal candidates.

This analysis requires the reconstruction of an extra track, compared to the $\mathcal{R}(D^*)$ analysis, which has studied the efficiency in great detail [9]. The uncertainty associated to the extra track reconstruction efficiency cancels to a large extent since the normalization channel also requires an extra track reconstruction. The $B^- \to D^{*+}\pi^-\pi^-\pi^-\pi^+$ control sample is used to compare the selection efficiency in data and simulation. For each selection criterion the relative efficiency is measured, using data around the known B^- mass [14]. A good agreement is found, except for the efficiency of the vertex detachment requirement, which deviates by 10% due to differences in the vertex resolution between data and simulation at 13 TeV. After correcting for such discrepancy, a

TABLE II. Summary of relative systematic uncertainties on $\kappa_{D_{1,2}^{**0}}$ related to the various identified sources.

Source	Systematic uncertainty [%]
Form factors	3.7
$D_2^*(2460)^0$ fraction	4.4
Finite size of the simulated samples—efficiency	4.3
Finite size of the simulated samples—templates	4.1
Variables and binning choices	5.0
$B^- \to D^{**0}(DK)^-$ background	3.6
Selection and analysis	2.0
Detachment requirement	4.0
WS background description	2.0
Total	11.4

systematic uncertainty of 2% is assigned due to the limited knowledge of the analysis selection efficiency, in line with what has been found in the $\mathcal{R}(D^*)$ analysis [9].

The background suppression due to the detachment requirement must be correctly described in simulation, so that the contamination of prompt background is correctly accounted in the fit. A comparison is made between the suppression factor in data and in simulation of the prompt $B^- \to D^{*+}\pi^-\pi^-\pi^-\pi^+$ peak when requiring 2, 3 or 4σ separation between the B^- and τ^- vertices. An agreement within 4% is observed and assigned as a systematic uncertainty. A key feature of this analysis is the modeling of the fake D^{**} background with data using the WS sample. The discrepancy between the observed background under the Δm peak and its estimation is less than 5% in the full Δm range (cf. Fig. 5). Weighting the WS background mass distribution within such limit leads to a signal yield change of 2%, which is assigned as the corresponding systematic uncertainty. Table II summarizes the systematic uncertainties for this measurement. The total uncertainty is the sum in quadrature of the individual components.

In order to improve the statistical precision of the normalization channel yield, the $B^- \to D^{*+}D_s^-\pi^-$ and $B^- \to D^{*+}D_s^{*-}(\to D_s^-\gamma)\pi^-$ contributions are summed. The respective yields, obtained after a sideband subtraction around the D_s^- mass peak, are 116 ± 11 and 177 ± 14. The ratio of the corresponding branching fractions has been measured by the LHCb Collaboration to be 1.31 ± 0.16 [16]. The efficiency ratio ϵ_R between the signal and normalization channels, is expected to be far away from unity because of the presence of the two neutrinos in the signal channel. It is measured to be $\epsilon_R = 0.38 \pm 0.02$ in the inclusive simulated sample, taking into account the slightly different efficiencies of the D_s^- and D_s^{*-} channels. Combining these informations in Eq. (1) gives

$$\frac{\mathcal{B}(B^- \to D_{1,2}^{**0}\tau^-\bar{\nu}_\tau)}{\mathcal{B}(B^- \to D_{1,2}^{**0}D_s^{(*)-})} = 0.19 \pm 0.04(\text{stat}) \pm 0.02(\text{syst}).$$

Using the branching fraction of the normalization channel from Ref. [16], $\mathcal{B}(B^- \to D_{1,2}^{**0}D_s^{(*)}) = (0.27 \pm 0.05)\%$, where $D_1(2420)^0$ and $D_2^*(2460)^0$ mesons decay to the $D^{*+}\pi^-$ final state, it follows that

$$\mathcal{B}(B^- \to D_{1,2}^{**0}\tau^-\bar{\nu}_\tau) \times \mathcal{B}(D_{1,2}^{**0} \to D^{*+}\pi^-) = (0.051 \pm 0.013(\text{stat}) \pm 0.006(\text{syst}) \pm 0.009(\text{ext}))\%,$$

where the last uncertainty accounts for the normalization channel branching fraction uncertainty. The branching fraction $\mathcal{B}(B^- \to D^{**0}\tau^-\bar{\nu}_\tau) \times \mathcal{B}(D^{**0} \to D^{*+}\pi^-) = [0.085 \pm 0.026(\text{stat}) \pm 0.009(\text{syst}) \pm 0.016(\text{ext})]\%$ corresponds to the average total D^{**0} yield in the two extreme cases where the fraction of the $D_1'(2400)^0$ component in the $D^{**0}\tau^-\bar{\nu}_\tau$ signal is assumed to be 0 or 100%, and the first uncertainty covers the variation of the total D^{**0} yield between these two cases. The branching fraction $\mathcal{B}(B^- \to D_{1,2}^{**0}\tau^-\bar{\nu}_\tau) \times \mathcal{B}(D_{1,2}^{**0} \to D^{*+}\pi^-)$ is found to be less than 0.094% at 90% CL in the first case. In the very unlikely case of a pure $D_1'(2400)^0\tau^-\bar{\nu}_\tau$ component, the result is $\mathcal{B}(B^- \to D_1'(2400)^0\tau^-\bar{\nu}_\tau) \times \mathcal{B}(D_1'(2400)^0 \to D^{*+}\pi^-) = [0.111 \pm 0.017(\text{stat}) \pm 0.010(\text{syst}) \pm 0.019(\text{ext})]\%$. Given that the branching fractions for the muonic B^--decay channels involving the $D_1(2420)^0$ and $D_2^*(2460)^0$ states are $(0.30 \pm 0.02)\%$ and $(0.10 \pm 0.02)\%$ [14], the following ratio is determined:

$$\mathcal{R}(D_{1,2}^{**0}) = 0.13 \pm 0.03(\text{stat}) \pm 0.01(\text{syst}) \pm 0.02(\text{ext}).$$

The measured ratio is compatible with the SM prediction of 0.09 ± 0.02 [41,42,48] and with assumptions made in the $\mathcal{R}(D^{(*)})$ measurements [3–12] on the $\mathcal{R}(D^{**})$ value. This implies that the observed deviation of $\mathcal{R}(D^{(*)})$ from the SM prediction is not likely to be due to a global underestimation of $B \to D^{**}\tau^-\bar{\nu}_\tau$ decays.

Regarding the $\mathcal{R}(D^*)$ measurement by LHCb Collaboration based on hadronic τ^- decays [9], and assuming a total of 9000 $\bar{B}^0 \to D^{*+}\tau^-\bar{\nu}_\tau$ decays in the full 9 fb^{-1} data sample, the expected value of the feed-down fraction of $B \to D^{**}\tau^-\bar{\nu}_\tau$ candidates in the fitted sample is estimated to be $(8.9 \pm 2.1)\%$, leading to an upper limit of 11.1% (13.1%) at the 90% (95%) confidence level. Taking into account the extra $(0.7 \pm 0.1)\%$ contribution arising from $\bar{B}_s^0 \to D_s^{**+}\tau^-\bar{\nu}_\tau$ decays and the uncertainty regarding the total signal yield, the total feed-down contribution is larger than the 3.5% rate used in Ref. [9], but compatible within 2.6σ. The corresponding shift in $\mathcal{R}(D^*)$ quoted there is well within one standard deviation.

In summary, evidence for the $B^- \to D^{**0}\tau^-\bar{\nu}_\tau$ channel is obtained with a significance of 3.5σ. The branching

fractions $\mathcal{B}(B^- \to D^{**0}_{1,2}\tau^-\bar{\nu}_\tau) \times \mathcal{B}(D^{**0}_{1,2} \to D^{*+}\pi^-)$ and the ratio $\mathcal{R}(D^{**0}_{1,2})$ are measured for the first time. The latter is found to be in good agreement with the SM prediction and consistent with the assumptions used in the various $\mathcal{R}(D^{(*)})$ measurements.

Acknowledgments—We express our gratitude to our colleagues in the CERN accelerator departments for the excellent performance of the LHC. We thank the technical and administrative staff at the LHCb institutes. We acknowledge support from CERN and from the following national agencies: ARC and ARDC (Australia); CAPES, CNPq, FAPERJ, and FINEP (Brazil); MOST and NSFC (China); CNRS/IN2P3 (France); BMBF, DFG, and MPG (Germany); INFN (Italy); NWO (Netherlands); MNiSW and NCN (Poland); MCID/IFA (Romania); MICIU and AEI (Spain); SNSF and State Secretariat for Education and Research (SER) (Switzerland); NASU (Ukraine); STFC (United Kingdom); DOE NP and NSF (USA). We acknowledge the computing resources that are provided by CERN, IN2P3 (France), KIT and DESY (Germany), INFN (Italy), Samenwerkende Universitaire Rekenfaciliteiten/ Cooperating University Computing Facilities (SURF) (Netherlands), Port d'Informació Científica (PIC) (Spain), Grid for Particle Physic (GridPP) (United Kingdom), CSCS (Switzerland), IFIN-HH (Romania), Centro Brasileiro de Pesquisas Físicas (CBPF) (Brazil), and Polish Worldwide LHC Computing Grid (Polish WLCG) (Poland). We are indebted to the communities behind the multiple open-source software packages on which we depend. Individual groups or members have received support from Key Research Program of Frontier Sciences of CAS, Chinese Academy of sciences President's International Fellowship Initiative(CAS PIFI), CAS CCEPP, Fundamental Research Funds for the Central Universities, and Sci. & Tech. Program of Guangzhou (China); Minciencias (Colombia); European Particle physics Latin-American NETwork (EPLANET), Marie Skłodowska-Curie Actions, ERC and NextGenerationEU (European Union); A*MIDEX, ANR, IPhU and Labex P2IO, and Région Auvergne-Rhône-Alpes (France); AvH Foundation (Germany); ICSC (Italy); Severo Ochoa and María de Maeztu Units of Excellence, GVA, XuntaGal, GENCAT, InTalent-Inditex and Prog. Atracción Talento CM (Spain); SRC (Sweden); the Leverhulme Trust, the Royal Society and UKRI (United Kingdom).

Data availability—The data that support the findings of this Letter are not publicly available. The data are available from the authors upon reasonable request. The plots in this publication are made available in Ref. [49].

[1] S. Fajfer, J. F. Kamenik, and I. Nisandzic, On the $B \to D^*\tau\bar{\nu}_\tau$ sensitivity to new physics, Phys. Rev. D **85**, 094025 (2012).

[2] J. Aebischer, G. Isidori, M. Pesut, B. A. Stefanek, and F. Wilsch, Confronting the vector leptoquark hypothesis with new low- and high-energy data, Eur. Phys. J. C **83**, 153 (2023).

[3] J. P. Lees *et al.* (*BABAR* Collaboration), Evidence for an excess of $\bar{B} \to D^{(*)}\tau^-\bar{\nu}_\tau$ decays, Phys. Rev. Lett. **109**, 101802 (2012).

[4] M. Huschle *et al.* (Belle Collaboration), Measurement of the branching ratio of $\bar{B} \to D^{(*)}\tau^-\bar{\nu}_\tau$ relative to $\bar{B} \to D^{(*)}\ell^-\bar{\nu}_\ell$ decays with hadronic tagging at Belle, Phys. Rev. D **92**, 072014 (2015).

[5] Y. Sato *et al.* (Belle Collaboration), Measurement of the branching ratio of $\bar{B}^0 \to D^{*+}\tau^-\bar{\nu}_\tau$ relative to $\bar{B}^0 \to D^{*+}\ell^-\bar{\nu}_\ell$ decays with a semileptonic tagging method, Phys. Rev. D **94**, 072007 (2016).

[6] S. Hirose *et al.* (Belle Collaboration), Measurement of the τ lepton polarization and $R(D^*)$ in the decay $\bar{B} \to D^*\tau^-\bar{\nu}_\tau$ with one-prong hadronic τ decays at Belle, Phys. Rev. D **97**, 012004 (2018).

[7] R. Aaij *et al.* (LHCb Collaboration), Measurement of the ratio of the $\mathcal{B}(B^0 \to D^{*-}\tau^+\nu_\tau)$ and $\mathcal{B}(B^0 \to D^{*-}\mu^+\nu_\mu)$ branching fractions using three-prong τ-lepton decays, Phys. Rev. Lett. **120**, 171802 (2018).

[8] R. Aaij *et al.* (LHCb Collaboration), Test of lepton flavor universality by the measurement of the $B^0 \to D^{*-}\tau^+\nu_\tau$ branching fraction using three-prong τ decays, Phys. Rev. D **97**, 072013 (2018).

[9] R. Aaij *et al.* (LHCb Collaboration), Test of lepton flavour universality using $B^0 \to D^{*-}\tau^+\nu_\tau$ decays, with hadronic τ channels, Phys. Rev. D **108**, 012018 (2023).

[10] R. Aaij *et al.* (LHCb Collaboration), Measurement of the ratio of branching fractions $\mathcal{R}(D^*)$ and $\mathcal{R}(D^0)$, Phys. Rev. Lett. **131**, 111802 (2023).

[11] R. Aaij *et al.* (LHCb Collaboration), Measurement of the branching fraction ratios $R(D^+)$ and $R(D^{*+})$ using muonic τ decays, Phys. Rev. Lett. **134**, 061801 (2025).

[12] I. Adachi *et al.* (Belle II Collaboration), Test of lepton flavor universality with a measurement of $R(D^*)$ using hadronic B tagging at the Belle II experiment, Phys. Rev. D **110**, 072020 (2024).

[13] Y. Amhis *et al.* (Heavy Flavour Averaging Group), Averages of b-hadron, c-hadron, and τ-lepton properties as of 2021, Phys. Rev. D **107**, 052008 (2023); results and plots updated to spring 2024 available at https://hflav.web.cern.ch.

[14] S. Navas *et al.* (Particle Data Group), Review of particle physics, Phys. Rev. D **110**, 030001 (2024).

[15] F. U. Bernlochner, M. Franco Sevilla, D. J. Robinson, and G. Wormser, Semitauonic b-hadron decays: A lepton flavor universality laboratory, Rev. Mod. Phys. **94**, 015003 (2022).

[16] R. Aaij *et al.* (LHCb Collaboration), Amplitude analysis and branching fraction measurement of $B^+ \to D^{*-}D_s^+\pi^+$ decays, J. High Energy Phys. 08 (2024) 165.

[17] A. A. Alves Jr. *et al.* (LHCb Collaboration), The LHCb detector at the LHC, J. Instrum. **3**, S08005 (2008).

[18] LHCb Collaboration, LHCb detector performance, Int. J. Mod. Phys. A **30**, 1530022 (2015).

[19] R. Aaij *et al.*, Performance of the LHCb vertex locator, J. Instrum. **9**, P09007 (2014).

[20] R. Aaij *et al.*, The LHCb trigger and its performance in 2011, J. Instrum. **8**, P04022 (2013).
[21] V. V. Gligorov and M. Williams, Efficient, reliable and fast high-level triggering using a bonsai boosted decision tree, J. Instrum. **8**, P02013 (2013).
[22] T. Likhomanenko, P. Ilten, E. Khairullin, A. Rogozhnikov, A. Ustyuzhanin, and M. Williams, LHCb topological trigger reoptimization, J. Phys. Conf. Ser. **664**, 082025 (2015).
[23] T. Sjöstrand, S. Mrenna, and P. Skands, PYTHIA 6.4 physics and manual, J. High Energy Phys. 05 (2006) 026; A brief introduction to PYTHIA 8.1, Comput. Phys. Commun. **178**, 852 (2008).
[24] I. Belyaev *et al.*, Handling of the generation of primary events in Gauss, the LHCb simulation framework, J. Phys. Conf. Ser. **331**, 032047 (2011).
[25] D. J. Lange, The EvtGen particle decay simulation package, Nucl. Instrum. Methods Phys. Res., Sect. A **462**, 152 (2001).
[26] N. Davidson, T. Przedzinski, and Z. Was, PHOTOS interface in C++: Technical and physics documentation, Comput. Phys. Commun. **199**, 86 (2016).
[27] N. Davidson, G. Nanava, T. Przedziński, E. Richter-Wąs, and Z. Wąs, Universal interface of Tauola technical and physics documentation, Comput. Phys. Commun. **183**, 821 (2012).
[28] I. M. Nugent, T. Przedziński, P. Roig, O. Shekhovtsova, and Z. Wąs, Resonance chiral Lagrangian currents and experimental data for $\tau^- \to \pi^-\pi^-\pi^+\nu_\tau$, Phys. Rev. D **88**, 093012 (2013).
[29] I. M. Nugent, Invariant mass spectra of $\tau^- \to h^-h^-h^+\nu_\tau$ decays, Nucl. Phys. B, Proc. Suppl. **253–255**, 38 (2014).
[30] J. Allison *et al.* (Geant4 Collaboration), Geant4 developments and applications, IEEE Trans. Nucl. Sci. **53**, 270 (2006); S. Agostinelli *et al.* (Geant4 Collaboration), Geant4: A simulation toolkit, Nucl. Instrum. Methods Phys. Res., Sect. A **506**, 250 (2003).
[31] M. Clemencic, G. Corti, S. Easo, C. R. Jones, S. Miglioranzi, M. Pappagallo, and P. Robbe, The LHCb simulation application, Gauss: Design, evolution and experience, J. Phys. Conf. Ser. **331**, 032023 (2011).
[32] R. Aaij *et al.* (LHCb Collaboration), Observation of the decay $\Lambda_b^0 \to \Lambda_c^+\tau^-\bar{\nu}_\tau$, Phys. Rev. Lett. **128**, 191803 (2021).
[33] M. Ablikim *et al.* (BESIII Collaboration), Precise measurements of branching fractions for D_s^+ meson decays to two pseudoscalar mesons, J. High Energy Phys. 08 (2020) 146.
[34] M. Ablikim *et al.* (BESIII Collaboration), Measurement of the branching fractions of $D_s^+ \to \eta' X$ and $D_s^+ \to \eta'\rho^+$ in $e^+e^- \to D_s^+D_s^-$, Phys. Lett. B **750**, 466 (2015).
[35] M. Ablikim *et al.* (BESIII Collaboration), Amplitude analysis of $D_s^+ \to \pi^+\pi^0\eta$ and first observation of the pure W-annihilation decays $D_s^+ \to a_0(980)^+\pi^0$ and $D_s^+ \to a_0(980)^0\pi^+$, Phys. Rev. Lett. **123**, 112001 (2019).
[36] M. Ablikim *et al.* (BESIII Collaboration), Amplitude analysis and branching-fraction measurement of $D_s^+ \to \pi^+\pi^0\eta'$, J. High Energy Phys. 04 (2022) 058.
[37] M. Ablikim *et al.* (BESIII Collaboration), Study of the decay $D_s^+ \to \pi^+\pi^+\pi^-\eta$ and observation of the W-annihilation decay $D_s^+ \to a_0(980)^+\rho^0$, Phys. Rev. D **104**, L071101 (2021).
[38] M. Ablikim *et al.* (BESIII Collaboration), Amplitude analysis and branching fraction measurement of $D_s^+ \to K^-K^+\pi^+\pi^+\pi^-$, J. High Energy Phys. 07 (2022) 051.
[39] M. Ablikim *et al.* (BESIII Collaboration), Observation of the W-annihilation decay $D_s^+ \to \omega\pi^+$ and evidence for $D_s^+ \to \omega K^+$, Phys. Rev. D **99**, 091101 (2019).
[40] M. Ablikim *et al.* (BESIII Collaboration), Measurement of the absolute branching fraction of the inclusive decay $D_s^+ \to \pi^+\pi^+\pi^- X$, Phys. Rev. D **108**, 032001 (2023).
[41] F. U. Bernlochner, Z. Ligeti, and D. J. Robinson, Model independent analysis of semileptonic B decays to D^{**} for arbitrary new physics, Phys. Rev. D **97**, 075011 (2018).
[42] N. Gubernari, A. Khodjamirian, R. Mandal, and T. Mannel, $B \to D_1(2420)$ and $B \to D_1'(2430)$ form factors from QCD light-cone sum rules, J. High Energy Phys. 05 (2022) 029.
[43] N. Isgur, D. Scora, B. Grinstein, and M. B. Wise, Semileptonic B and D decays in the quark model, Phys. Rev. D **39**, 799 (1989).
[44] A. K. Leibovich, Z. Ligeti, I. W. Stewart, and M. B. Wise, Semileptonic B decays to excited charmed mesons, Phys. Rev. D **57**, 308 (1998).
[45] F. U. Bernlochner, S. Duell, Z. Ligeti, M. Papucci, and D. J. Robinson, Das ist der HAMMER: Consistent new physics interpretations of semileptonic decays, Eur. Phys. J. C **80**, 883 (2020).
[46] B. Efron, Bootstrap methods: Another look at the jackknife, Ann. Stat. **7**, 1 (1979).
[47] R. Aaij *et al.* (LHCb Collaboration), Measurement of the D^* longitudinal polarisation in $B^0 \to D^{*-}\tau^+\nu_\tau$ decays, Phys. Rev. D **110**, 092007 (2024).
[48] A. L. Yaouanc, J.-P. Leroy, and P. Roudeau, A model for NL and SL decays by $\bar{B}^0 \to D^{**}$ transitions with $BR(j = 1/2) \ll BR(j = 3/2)$ using the *LLSW* scheme, Phys. Rev. D **105**, 013004 (2022).
[49] https://cds.cern.ch/record/2922701

End Matter

In order to ascertain whether genuine $B \to D^{**0}\bar{D}^0X$ events are present when associated to fully reconstructed $\bar{D}^0$ candidates, a sample of events combining fully reconstructed $\bar{D}^0$ and D^{**0} candidates is selected. Candidate $\bar{D}^0$ mesons are reconstructed in the $K^+\pi^-\pi^-\pi^+$ mode, requiring the presence of an extra kaon originating from the three pion vertex. Figure 4 shows the Δm distribution for the D^{**0} candidates reconstructed together with a $\bar{D}^0$ meson. In the distribution of the mass difference between the $D_1(2420)^0$ and D^{*+} mesons, only a small hint of D^{**0} candidates is observed around 410 MeV/c^2. This demonstrates that the vast majority of these events contains fake D^{**0} candidates.

In order to check that the fake D^{**0} background can be well described by the D^{**0} WS sample, a study is performed using a simulated sample of inclusive b-hadron decays to final states containing a D^{*+} meson and three additional charged pions. The mass distribution of the

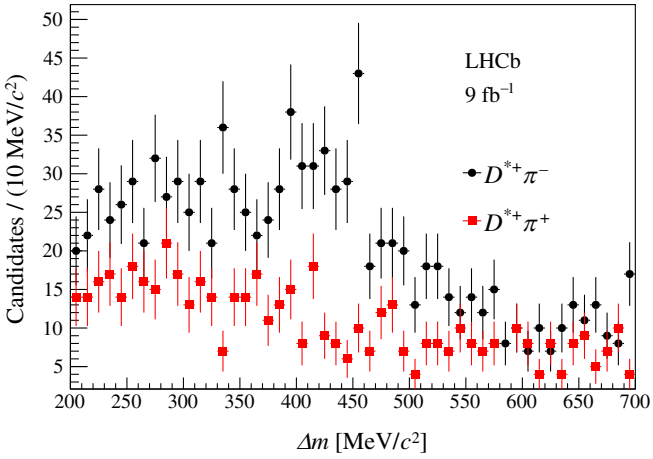

FIG. 4. Distribution of the Δm mass difference for $B^- \to D^{*+}\pi^-\bar{D}^0(K^-)$ candidates, with $\bar{D}^0$ reconstructed in the $K^+\pi^-\pi^-\pi^+$ final state. Here the K^- meson is not reconstructed. The black (red) points correspond to the RS (WS) sample.

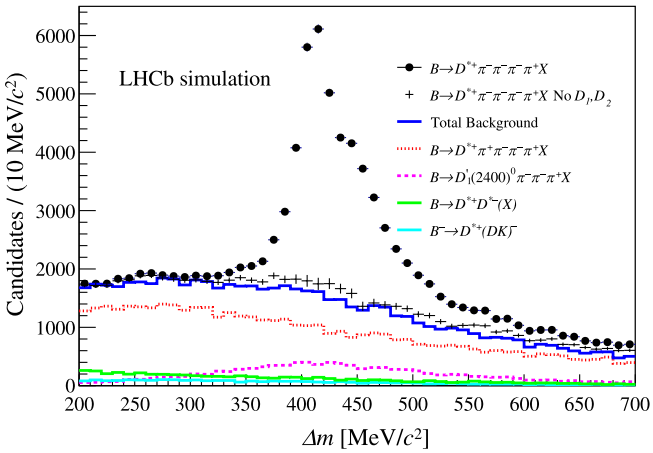

FIG. 5. Distribution of the Δm mass difference for all selected D^{**0} candidates in the inclusive simulated sample (black circles) compared to the WS sample extracted from the same dataset. The background under the Δm peak in RS sample (black crosses) corresponds to RS simulated events not containing a $D_1(2420)^0$ or $D_2^*(2460)^0$ meson. A good agreement is found between this component and the (dark blue) total background estimate which is the sum of the WS candidates plus RS candidates containing either a $D_1'(2400)^0$ meson, a $D^{*+}D^{*-}$ pair, or three-body $D^{*+}(DK)^-$ in the final state.

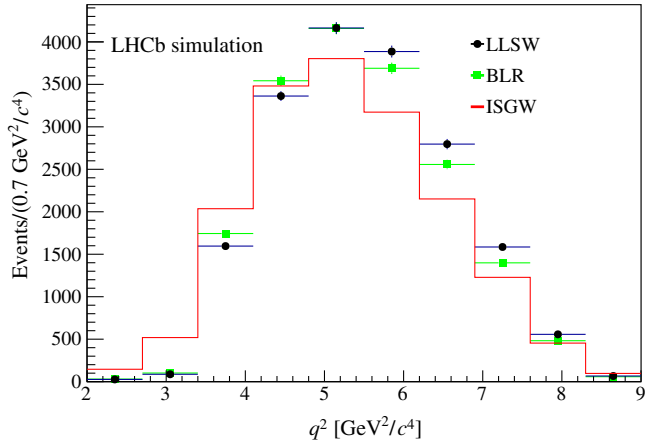

FIG. 6. Distribution of the q^2 observable for simulated $B^- \to D_1(2420)^0\tau^-\bar{\nu}_\tau$ decays corresponding to the BLR [41], LLSW [44], and ISGW2 [43] form-factor models.

background under the D^{**0} peak in the RS sample is compared to that of the WS candidates in the same simulated sample. As can be seen in Fig. 5, a good agreement is found, validating the procedure.

Three different theoretical models (BLR [41], LLSW [44], and ISGW2 [43]) can be used to describe the semileptonic $B \to D^{**}\tau\nu$ decays. Figure 6 displays the q^2 distribution for each model, showing that the BLR and LLSW models are rather similar, while the ISGW2 model predicts a q^2 distribution shifted toward lower values.

R. Aaij,[38] A. S. W. Abdelmotteleb,[57] C. Abellan Beteta,[51] F. Abudinén,[57] T. Ackernley,[61] A. A. Adefisoye,[69] B. Adeva,[47] M. Adinolfi,[55] P. Adlarson,[82] C. Agapopoulou,[14] C. A. Aidala,[83] Z. Ajaltouni,[11] S. Akar,[66] K. Akiba,[38] P. Albicocco,[28] J. Albrecht,[19,b] F. Alessio,[49] Z. Aliouche,[63] P. Alvarez Cartelle,[56] R. Amalric,[16] S. Amato,[3] J. L. Amey,[55] Y. Amhis,[14] L. An,[6] L. Anderlini,[27] M. Andersson,[51] A. Andreianov,[44] P. Andreola,[51] M. Andreotti,[26] D. Andreou,[69] A. Anelli,[31,c] D. Ao,[7] F. Archilli,[37,d] M. Argenton,[26] S. Arguedas Cuendis,[9,49] A. Artamonov,[44] M. Artuso,[69] E. Aslanides,[13] R. Ataíde Da Silva,[50] M. Atzeni,[65] B. Audurier,[12] D. Bacher,[64] I. Bachiller Perea,[10] S. Bachmann,[22] M. Bachmayer,[50] J. J. Back,[57] P. Baladron Rodriguez,[47] V. Balagura,[15] A. Balboni,[26] W. Baldini,[26] L. Balzani,[19] H. Bao,[7] J. Baptista de Souza Leite,[61] C. Barbero Pretel,[47,12] M. Barbetti,[27] I. R. Barbosa,[70] R. J. Barlow,[63] M. Barnyakov,[25] S. Barsuk,[14] W. Barter,[59] M. Bartolini,[56] J. Bartz,[69] J. M. Basels,[17] S. Bashir,[40] G. Bassi,[35,e] B. Batsukh,[5] P. B. Battista,[14] A. Bay,[50] A. Beck,[57] M. Becker,[19] F. Bedeschi,[35] I. B. Bediaga,[2] N. A. Behling,[19] S. Belin,[47] K. Belous,[44] I. Belov,[29] I. Belyaev,[36] G. Benane,[13] G. Bencivenni,[28] E. Ben-Haim,[16] A. Berezhnoy,[44] R. Bernet,[51] S. Bernet Andres,[45] A. Bertolin,[33] C. Betancourt,[51] F. Betti,[59] J. Bex,[56] Ia. Bezshyiko,[51] J. Bhom,[41] M. S. Bieker,[19] N. V. Biesuz,[26] P. Billoir,[16] A. Biolchini,[38] M. Birch,[62] F. C. R. Bishop,[10] A. Bitadze,[63] A. Bizzeti, T. Blake,[57] F. Blanc,[50] J. E. Blank,[19] S. Blusk,[69] V. Bocharnikov,[44] J. A. Boelhauve,[19] O. Boente Garcia,[15] T. Boettcher,[66] A. Bohare,[59] A. Boldyrev,[44] C. S. Bolognani,[79] R. Bolzonella,[26,f] R. B. Bonacci,[1] N. Bondar,[44] A. Bordelius,[49] F. Borgato,[33,g] S. Borghi,[63] M. Borsato,[31,c] J. T. Borsuk,[41] S. A. Bouchiba,[50] M. Bovill,[64] T. J. V. Bowcock,[61] A. Boyer,[49] C. Bozzi,[26] A. Brea Rodriguez,[50] N. Breer,[19] J. Brodzicka,[41] A. Brossa Gonzalo,[47,a] J. Brown,[61] D. Brundu,[32] E. Buchanan,[59] A. Buonaura,[51] L. Buonincontri,[33,g] A. T. Burke,[63] C. Burr,[49] J. S. Butter,[56] J. Buytaert,[49] W. Byczynski,[49] S. Cadeddu,[32] H. Cai,[74] A. Caillet,[16] R. Calabrese,[26,f] S. Calderon Ramirez,[9] L. Calefice,[46] S. Cali,[28] M. Calvi,[31,c] M. Calvo Gomez,[45] P. Camargo Magalhaes,[2,h] J. I. Cambon Bouzas,[47] P. Campana,[28] D. H. Campora Perez,[79] A. F. Campoverde Quezada,[7] S. Capelli,[31] L. Capriotti,[26] R. Caravaca-Mora,[9] A. Carbone,[25,i] L. Carcedo Salgado,[47] R. Cardinale,[29,j] A. Cardini,[32] P. Carniti,[31,c] L. Carus,[22] A. Casais Vidal,[65] R. Caspary,[22] G. Casse,[61] M. Cattaneo,[49] G. Cavallero,[26,49] V. Cavallini,[26,f] S. Celani,[22] D. Cervenkov,[64] S. Cesare,[30,k] A. J. Chadwick,[61] I. Chahrour,[83] M. Charles,[16] Ph. Charpentier,[49] E. Chatzianagnostou,[38] M. Chefdeville,[10] C. Chen,[13] S. Chen,[5] Z. Chen,[7] A. Chernov,[41] S. Chernyshenko,[53] X. Chiotopoulos,[79] V. Chobanova,[81] S. Cholak,[50] M. Chrzaszcz,[41] A. Chubykin,[44] V. Chulikov,[28] P. Ciambrone,[28] X. Cid Vidal,[47] G. Ciezarek,[49] P. Cifra,[49] P. E. L. Clarke,[59] M. Clemencic,[49] H. V. Cliff,[56] J. Closier,[49] C. Cocha Toapaxi,[22] V. Coco,[49] J. Cogan,[13] E. Cogneras,[11] L. Cojocariu,[43] S. Collaviti,[50] P. Collins,[49] T. Colombo,[49] M. Colonna,[19] A. Comerma-Montells,[46] L. Congedo,[24] A. Contu,[32] N. Cooke,[60] I. Corredoira,[47] A. Correia,[16] G. Corti,[49] J. Cottee Meldrum,[55] B. Couturier,[49] D. C. Craik,[51] M. Cruz Torres,[2,l] E. Curras Rivera,[50] R. Currie,[59] C. L. Da Silva,[68] S. Dadabaev,[44] L. Dai,[71] X. Dai,[6] E. Dall'Occo,[49] J. Dalseno,[47] C. D'Ambrosio,[49] J. Daniel,[11] A. Danilina,[44] P. d'Argent,[24] G. Darze,[3] A. Davidson,[57] J. E. Davies,[63] A. Davis,[63] O. De Aguiar Francisco,[63] C. De Angelis,[32,m] F. De Benedetti,[49] J. de Boer,[38] K. De Bruyn,[78] S. De Capua,[63] M. De Cian,[22] U. De Freitas Carneiro Da Graca,[2,n] E. De Lucia,[28] J. M. De Miranda,[2] L. De Paula,[3] M. De Serio,[24,o] P. De Simone,[28] F. De Vellis,[19] J. A. de Vries,[79] F. Debernardis,[24] D. Decamp,[10] V. Dedu,[13] S. Dekkers,[1] L. Del Buono,[16] B. Delaney,[65] H.-P. Dembinski,[19] J. Deng,[8] V. Denysenko,[51] O. Deschamps,[11] F. Dettori,[32,m] B. Dey,[77] P. Di Nezza,[28] I. Diachkov,[44] S. Didenko,[44] S. Ding,[69] L. Dittmann,[22] V. Dobishuk,[53]

A. D. Docheva,[60] C. Dong,[4,p] A. M. Donohoe,[23] F. Dordei,[32] A. C. dos Reis,[2] A. D. Dowling,[69] W. Duan,[72] P. Duda,[80] M. W. Dudek,[41] L. Dufour,[49] V. Duk,[34] P. Durante,[49] M. M. Duras,[80] J. M. Durham,[68] O. D. Durmus,[77] A. Dziurda,[41] A. Dzyuba,[44] S. Easo,[58] E. Eckstein,[18] U. Egede,[1] A. Egorychev,[44] V. Egorychev,[44] S. Eisenhardt,[59] E. Ejopu,[63] L. Eklund,[82] M. Elashri,[66] J. Ellbracht,[19] S. Ely,[62] A. Ene,[43] J. Eschle,[69] S. Esen,[22] T. Evans,[63] F. Fabiano,[32,m] L. N. Falcao,[2] Y. Fan,[7] B. Fang,[7] L. Fantini,[34,49,q] M. Faria,[50] K. Farmer,[59] D. Fazzini,[31,c] L. Felkowski,[80] M. Feng,[5,7] M. Feo,[19] A. Fernandez Casani,[48] M. Fernandez Gomez,[47] A. D. Fernez,[67] F. Ferrari,[25,i] F. Ferreira Rodrigues,[3] M. Ferrillo,[51] M. Ferro-Luzzi,[49] S. Filippov,[44] R. A. Fini,[24] M. Fiorini,[26,f] M. Firlej,[40] K. L. Fischer,[64] D. S. Fitzgerald,[83] C. Fitzpatrick,[63] T. Fiutowski,[40] F. Fleuret,[15] M. Fontana,[25] L. F. Foreman,[63] R. Forty,[49] D. Foulds-Holt,[56] V. Franco Lima,[3] M. Franco Sevilla,[67] M. Frank,[49] E. Franzoso,[26,f] G. Frau,[63] C. Frei,[49] D. A. Friday,[63] J. Fu,[7] Q. Führing,[19,56,b] Y. Fujii,[1] T. Fulghesu,[16] E. Gabriel,[38] G. Galati,[24] M. D. Galati,[38] A. Gallas Torreira,[47] D. Galli,[25,i] S. Gambetta,[59] M. Gandelman,[3] P. Gandini,[30] B. Ganie,[63] H. Gao,[7] R. Gao,[64] T. Q. Gao,[56] Y. Gao,[8] Y. Gao,[6] Y. Gao,[8] L. M. Garcia Martin,[50] P. Garcia Moreno,[46] J. García Pardiñas,[49] P. Gardner,[67] K. G. Garg,[8] L. Garrido,[46] C. Gaspar,[49] R. E. Geertsema,[38] L. L. Gerken,[19] E. Gersabeck,[63] M. Gersabeck,[20] T. Gershon,[57] S. Ghizzo,[29,j] Z. Ghorbanimoghaddam,[55] L. Giambastiani,[33,g] F. I. Giasemis,[16,r] V. Gibson,[56] H. K. Giemza,[42] A. L. Gilman,[64] M. Giovannetti,[28] A. Gioventù,[46] L. Girardey,[63,58] P. Gironella Gironell,[46] C. Giugliano,[26,f] M. A. Giza,[41] E. L. Gkougkousis,[62] F. C. Glaser,[14,22] V. V. Gligorov,[16,49] C. Göbel,[70] E. Golobardes,[45] D. Golubkov,[44] A. Golutvin,[62,49,44] S. Gomez Fernandez,[46] W. Gomulka,[40] F. Goncalves Abrantes,[64] M. Goncerz,[41] G. Gong,[4,p] J. A. Gooding,[19] I. V. Gorelov,[44] C. Gotti,[31] J. P. Grabowski,[18] L. A. Granado Cardoso,[49] E. Graugés,[46] E. Graverini,[50,s] L. Grazette,[57] G. Graziani, A. T. Grecu,[43] L. M. Greeven,[38] N. A. Grieser,[66] L. Grillo,[60] S. Gromov,[44] C. Gu,[15] M. Guarise,[26] L. Guerry,[11] M. Guittiere,[14] V. Guliaeva,[44] P. A. Günther,[22] A.-K. Guseinov,[50] E. Gushchin,[44] Y. Guz,[6,49,44] T. Gys,[49] K. Habermann,[18] T. Hadavizadeh,[1] C. Hadjivasiliou,[67] G. Haefeli,[50] C. Haen,[49] M. Hajheidari,[49] G. Hallett,[57] M. M. Halvorsen,[49] P. M. Hamilton,[67] J. Hammerich,[61] Q. Han,[8] X. Han,[22,49] S. Hansmann-Menzemer,[22] L. Hao,[7] N. Harnew,[64] T. H. Harris,[1] M. Hartmann,[14] S. Hashmi,[40] J. He,[7,t] F. Hemmer,[49] C. Henderson,[66] R. D. L. Henderson,[1,57] A. M. Hennequin,[49] K. Hennessy,[61] L. Henry,[50] J. Herd,[62] P. Herrero Gascon,[22] J. Heuel,[17] A. Hicheur,[3] G. Hijano Mendizabal,[51] J. Horswill,[63] R. Hou,[8] Y. Hou,[11] N. Howarth,[61] J. Hu,[72] W. Hu,[6] X. Hu,[4,p] W. Huang,[7] W. Hulsbergen,[38] R. J. Hunter,[57] M. Hushchyn,[44] D. Hutchcroft,[61] M. Idzik,[40] D. Ilin,[44] P. Ilten,[66] A. Inglessi,[44] A. Iniukhin,[44] A. Ishteev,[44] K. Ivshin,[44] R. Jacobsson,[49] H. Jage,[17] S. J. Jaimes Elles,[75,49,48] S. Jakobsen,[49] E. Jans,[38] B. K. Jashal,[48] A. Jawahery,[67,49] V. Jevtic,[19,b] E. Jiang,[67] X. Jiang,[5,7] Y. Jiang,[7] Y. J. Jiang,[6] M. John,[64] A. John Rubesh Rajan,[23] D. Johnson,[54] C. R. Jones,[56] T. P. Jones,[57] S. Joshi,[42] B. Jost,[49] J. Juan Castella,[56] N. Jurik,[49] I. Juszczak,[41] D. Kaminaris,[50] S. Kandybei,[52] M. Kane,[59] Y. Kang,[4,p] C. Kar,[11] M. Karacson,[49] D. Karpenkov,[44] A. Kauniskangas,[50] J. W. Kautz,[66] M. K. Kazanecki,[41] F. Keizer,[49] M. Kenzie,[56] T. Ketel,[38] B. Khanji,[69] A. Kharisova,[44] S. Kholodenko,[35,49] G. Khreich,[14] T. Kirn,[17] V. S. Kirsebom,[31,c] O. Kitouni,[65] S. Klaver,[39] N. Kleijne,[35,e] K. Klimaszewski,[42] M. R. Kmiec,[42] S. Koliiev,[53] L. Kolk,[19] A. Konoplyannikov,[44] P. Kopciewicz,[40,49] P. Koppenburg,[38] M. Korolev,[44] I. Kostiuk,[38] O. Kot,[53] S. Kotriakhova, A. Kozachuk,[44] P. Kravchenko,[44] L. Kravchuk,[44] M. Kreps,[57] P. Krokovny,[44] W. Krupa,[69] W. Krzemien,[42] O. Kshyvanskyi,[53] S. Kubis,[80] M. Kucharczyk,[41] V. Kudryavtsev,[44] E. Kulikova,[44] A. Kupsc,[82] B. Kutsenko,[13] D. Lacarrere,[49] P. Laguarta Gonzalez,[46] A. Lai,[32] A. Lampis,[32] D. Lancierini,[56] C. Landesa Gomez,[47] J. J. Lane,[1] R. Lane,[55] G. Lanfranchi,[28] C. Langenbruch,[22] J. Langer,[19] O. Lantwin,[44] T. Latham,[57] F. Lazzari,[35,s] C. Lazzeroni,[54] R. Le Gac,[13] H. Lee,[61] R. Lefèvre,[11] A. Leflat,[44] S. Legotin,[44] M. Lehuraux,[57] E. Lemos Cid,[49] O. Leroy,[13] T. Lesiak,[41] E. D. Lesser,[49] B. Leverington,[22] A. Li,[4,p] C. Li,[13] H. Li,[72] K. Li,[8] L. Li,[63] M. Li,[8] P. Li,[7] P.-R. Li,[73] Q. Li,[5,7] S. Li,[8] T. Li,[5,u] T. Li,[72] Y. Li,[8] Y. Li,[5] Z. Lian,[4,p] X. Liang,[69] S. Libralon,[48] C. Lin,[7] T. Lin,[58] R. Lindner,[49] H. Linton,[62] V. Lisovskyi,[50] R. Litvinov,[32,49] F. L. Liu,[1] G. Liu,[72] K. Liu,[73] S. Liu,[5,7] W. Liu,[8] Y. Liu,[59] Y. Liu,[73] Y. L. Liu,[62] A. Lobo Salvia,[46] A. Loi,[32] T. Long,[56] J. H. Lopes,[3] A. Lopez Huertas,[46] S. López Soliño,[47] Q. Lu,[15] C. Lucarelli,[27] D. Lucchesi,[33,g] M. Lucio Martinez,[79] V. Lukashenko,[38,53] Y. Luo,[6] A. Lupato,[33,v] E. Luppi,[26,f] K. Lynch,[23] X.-R. Lyu,[7] G. M. Ma,[4,p] S. Maccolini,[19] F. Machefert,[14] F. Maciuc,[43] B. Mack,[69] I. Mackay,[64] L. M. Mackey,[69] L. R. Madhan Mohan,[56] M. J. Madurai,[54] A. Maevskiy,[44] D. Magdalinski,[38] D. Maisuzenko,[44]

M. W. Majewski,[40] J. J. Malczewski,[41] S. Malde,[64] L. Malentacca,[49] A. Malinin,[44] T. Maltsev,[44] G. Manca,[32,m] G. Mancinelli,[13] C. Mancuso,[30,14,k] R. Manera Escalero,[46] F. M. Manganella,[37] D. Manuzzi,[25] D. Marangotto,[30,k] J. F. Marchand,[10] R. Marchevski,[50] U. Marconi,[25] E. Mariani,[16] S. Mariani,[49] C. Marin Benito,[46,49] J. Marks,[22] A. M. Marshall,[55] L. Martel,[64] G. Martelli,[34,q] G. Martellotti,[36] L. Martinazzoli,[49] M. Martinelli,[31,c] D. Martinez Gomez,[78] D. Martinez Santos,[81] F. Martinez Vidal,[48] A. Martorell i Granollers,[45] A. Massafferri,[2] R. Matev,[49] A. Mathad,[49] V. Matiunin,[44] C. Matteuzzi,[69] K. R. Mattioli,[15] A. Mauri,[62] E. Maurice,[15] J. Mauricio,[46] P. Mayencourt,[50] J. Mazorra de Cos,[48] M. Mazurek,[42] M. McCann,[62] L. Mcconnell,[23] T. H. McGrath,[63] N. T. McHugh,[60] A. McNab,[63] R. McNulty,[23] B. Meadows,[66] G. Meier,[19] D. Melnychuk,[42] F. M. Meng,[4,p] M. Merk,[38,79] A. Merli,[50] L. Meyer Garcia,[67] D. Miao,[5,7] H. Miao,[7] M. Mikhasenko,[76] D. A. Milanes,[75] A. Minotti,[31,c] E. Minucci,[28] T. Miralles,[11] B. Mitreska,[19] D. S. Mitzel,[19] A. Modak,[58] R. A. Mohammed,[64] R. D. Moise,[17] S. Mokhnenko,[44] E. F. Molina Cardenas,[83] T. Mombächer,[49] M. Monk,[57,1] S. Monteil,[11] A. Morcillo Gomez,[47] G. Morello,[28] M. J. Morello,[35,e] M. P. Morgenthaler,[22] J. Moron,[40] W. Morren,[38] A. B. Morris,[49] A. G. Morris,[13] R. Mountain,[69] H. Mu,[4,p] Z. M. Mu,[6] E. Muhammad,[57] F. Muheim,[59] M. Mulder,[78] K. Müller,[51] F. Muñoz-Rojas,[9] R. Murta,[62] P. Naik,[61] T. Nakada,[50] R. Nandakumar,[58] T. Nanut,[49] I. Nasteva,[3] M. Needham,[59] N. Neri,[30,k] S. Neubert,[18] N. Neufeld,[49] P. Neustroev,[44] J. Nicolini,[19,14] D. Nicotra,[79] E. M. Niel,[49] N. Nikitin,[44] Q. Niu,[73] P. Nogarolli,[3] P. Nogga,[18] C. Normand,[55] J. Novoa Fernandez,[47] G. Nowak,[66] C. Nunez,[83] H. N. Nur,[60] A. Oblakowska-Mucha,[40] V. Obraztsov,[44] T. Oeser,[17] S. Okamura,[26,f] A. Okhotnikov,[44] O. Okhrimenko,[53] R. Oldeman,[32,m] F. Oliva,[59] M. Olocco,[19] C. J. G. Onderwater,[79] R. H. O'Neil,[59] D. Osthues,[19] J. M. Otalora Goicochea,[3] P. Owen,[51] A. Oyanguren,[48] O. Ozcelik,[59] F. Paciolla,[35,w] A. Padee,[42] K. O. Padeken,[18] B. Pagare,[57] P. R. Pais,[22] T. Pajero,[49] A. Palano,[24] M. Palutan,[28] X. Pan,[4,p] G. Panshin,[44] L. Paolucci,[57] A. Papanestis,[58,49] M. Pappagallo,[24,o] L. L. Pappalardo,[26,f] C. Pappenheimer,[66] C. Parkes,[63] D. Parmar,[76] B. Passalacqua,[26,f] G. Passaleva,[27] D. Passaro,[35,e] A. Pastore,[24] M. Patel,[62] J. Patoc,[64] C. Patrignani,[25,i] A. Paul,[69] C. J. Pawley,[79] A. Pellegrino,[38] J. Peng,[5,7] M. Pepe Altarelli,[28] S. Perazzini,[25] D. Pereima,[44] H. Pereira Da Costa,[68] A. Pereiro Castro,[47] P. Perret,[11] A. Perrevoort,[78] A. Perro,[49,13] M. J. Peters,[66] K. Petridis,[55] A. Petrolini,[29,j] J. P. Pfaller,[66] H. Pham,[69] L. Pica,[35,e] M. Piccini,[34] L. Piccolo,[32] B. Pietrzyk,[10] G. Pietrzyk,[14] D. Pinci,[36] F. Pisani,[49] M. Pizzichemi,[31,49,c] V. M. Placinta,[43] M. Plo Casasus,[47] T. Poeschl,[49] F. Polci,[16,49] M. Poli Lener,[28] A. Poluektov,[13] N. Polukhina,[44] I. Polyakov,[44] E. Polycarpo,[3] S. Ponce,[49] D. Popov,[7] S. Poslavskii,[44] K. Prasanth,[59] C. Prouve,[81] D. Provenzano,[32,m] V. Pugatch,[53] G. Punzi,[35,s] S. Qasim,[51] Q. Q. Qian,[6] W. Qian,[7] N. Qin,[4,p] S. Qu,[4,p] R. Quagliani,[49] R. I. Rabadan Trejo,[57] J. H. Rademacker,[55] M. Rama,[35] M. Ramírez García,[83] V. Ramos De Oliveira,[70] M. Ramos Pernas,[57] M. S. Rangel,[3] F. Ratnikov,[44] G. Raven,[39] M. Rebollo De Miguel,[48] F. Redi,[30,v] J. Reich,[55] F. Reiss,[63] Z. Ren,[7] P. K. Resmi,[64] R. Ribatti,[50] G. Ricart,[15,12] D. Riccardi,[35,e] S. Ricciardi,[58] K. Richardson,[65] M. Richardson-Slipper,[59] K. Rinnert,[61] P. Robbe,[14,49] G. Robertson,[60] E. Rodrigues,[61] A. Rodriguez Alvarez,[46] E. Rodriguez Fernandez,[47] J. A. Rodriguez Lopez,[75] E. Rodriguez Rodriguez,[47] J. Roensch,[19] A. Rogachev,[44] A. Rogovskiy,[58] D. L. Rolf,[49] P. Roloff,[49] V. Romanovskiy,[66] A. Romero Vidal,[47] G. Romolini,[26] F. Ronchetti,[50] T. Rong,[6] M. Rotondo,[28] S. R. Roy,[22] M. S. Rudolph,[69] M. Ruiz Diaz,[22] R. A. Ruiz Fernandez,[47] J. Ruiz Vidal,[82,x] A. Ryzhikov,[44] J. Ryzka,[40] J. J. Saavedra-Arias,[9] J. J. Saborido Silva,[47] R. Sadek,[15] N. Sagidova,[44] D. Sahoo,[77] N. Sahoo,[54] B. Saitta,[32,m] M. Salomoni,[31,49,c] I. Sanderswood,[48] R. Santacesaria,[36] C. Santamarina Rios,[47] M. Santimaria,[28,49] L. Santoro,[2] E. Santovetti,[37] A. Saputi,[26,49] D. Saranin,[44] A. Sarnatskiy,[78] G. Sarpis,[59] M. Sarpis,[63] C. Satriano,[36,y] A. Satta,[37] M. Saur,[6] D. Savrina,[44] H. Sazak,[17] F. Sborzacchi,[49,28] L. G. Scantlebury Smead,[64] A. Scarabotto,[19] S. Schael,[17] S. Scherl,[61] M. Schiller,[60] H. Schindler,[49] M. Schmelling,[21] B. Schmidt,[49] S. Schmitt,[17] H. Schmitz,[18] O. Schneider,[50] A. Schopper,[49] N. Schulte,[19] S. Schulte,[50] M. H. Schune,[14] R. Schwemmer,[49] G. Schwering,[17] B. Sciascia,[28] A. Sciuccati,[49] I. Segal,[76] S. Sellam,[47] A. Semennikov,[44] T. Senger,[51] M. Senghi Soares,[39] A. Sergi,[29,j] N. Serra,[51] L. Sestini,[33] A. Seuthe,[19] Y. Shang,[6] D. M. Shangase,[83] M. Shapkin,[44] R. S. Sharma,[69] I. Shchemerov,[44] L. Shchutska,[50] T. Shears,[61] L. Shekhtman,[44] Z. Shen,[6] S. Sheng,[5,7] V. Shevchenko,[44] B. Shi,[7] Q. Shi,[7] Y. Shimizu,[14] E. Shmanin,[25] R. Shorkin,[44] J. D. Shupperd,[69] R. Silva Coutinho,[69] G. Simi,[33,g] S. Simone,[24,o] N. Skidmore,[57] T. Skwarnicki,[69] M. W. Slater,[54] J. C. Smallwood,[64] E. Smith,[65] K. Smith,[68] M. Smith,[62] A. Snoch,[38] L. Soares Lavra,[59] M. D. Sokoloff,[66]

F. J. P. Soler,[60] A. Solomin,[44,55] A. Solovev,[44] I. Solovyev,[44] N. S. Sommerfeld,[18] R. Song,[1] Y. Song,[50] Y. Song,[4,p] Y. S. Song,[6] F. L. Souza De Almeida,[69] B. Souza De Paula,[3] E. Spadaro Norella,[29,j] E. Spedicato,[25] J. G. Speer,[19] E. Spiridenkov,[44] P. Spradlin,[60] V. Sriskaran,[49] F. Stagni,[49] M. Stahl,[49] S. Stahl,[49] S. Stanislaus,[64] E. N. Stein,[49] O. Steinkamp,[51] O. Stenyakin,[44] H. Stevens,[19] D. Strekalina,[44] Y. Su,[7] F. Suljik,[64] J. Sun,[32] L. Sun,[74] D. Sundfeld,[2] W. Sutcliffe,[51] P. N. Swallow,[54] K. Swientek,[40] F. Swystun,[56] A. Szabelski,[42] T. Szumlak,[40] Y. Tan,[4,p] Y. Tang,[74] M. D. Tat,[64] A. Terentev,[44] F. Terzuoli,[35,49,w] F. Teubert,[49] E. Thomas,[49] D. J. D. Thompson,[54] H. Tilquin,[62] V. Tisserand,[11] S. T'Jampens,[10] M. Tobin,[5,49] L. Tomassetti,[26,f] G. Tonani,[30,49,k] X. Tong,[6] D. Torres Machado,[2] L. Toscano,[19] D. Y. Tou,[4,p] C. Trippl,[45] G. Tuci,[22] N. Tuning,[38] L. H. Uecker,[22] A. Ukleja,[40] D. J. Unverzagt,[22] B. Urbach,[59] E. Ursov,[44] A. Usachov,[39] A. Ustyuzhanin,[44] U. Uwer,[22] V. Vagnoni,[25] V. Valcarce Cadenas,[47] G. Valenti,[25] N. Valls Canudas,[49] H. Van Hecke,[68] E. van Herwijnen,[62] C. B. Van Hulse,[47,z] R. Van Laak,[50] M. van Veghel,[38] G. Vasquez,[51] R. Vazquez Gomez,[46] P. Vazquez Regueiro,[47] C. Vázquez Sierra,[47] S. Vecchi,[26] J. J. Velthuis,[55] M. Veltri,[27,aa] A. Venkateswaran,[50] M. Verdoglia,[32] M. Vesterinen,[57] D. Vico Benet,[64] P. Vidrier Villalba,[46] M. Vieites Diaz,[49] X. Vilasis-Cardona,[45] E. Vilella Figueras,[61] A. Villa,[25] P. Vincent,[16] F. C. Volle,[54] D. vom Bruch,[13] N. Voropaev,[44] K. Vos,[79] C. Vrahas,[59] J. Wagner,[19] J. Walsh,[35] E. J. Walton,[1,57] G. Wan,[6] C. Wang,[22] G. Wang,[8] H. Wang,[73] J. Wang,[6] J. Wang,[5] J. Wang,[4,p] J. Wang,[74] M. Wang,[30] N. W. Wang,[7] R. Wang,[55] X. Wang,[8] X. Wang,[72] X. W. Wang,[62] Y. Wang,[6] Y. W. Wang,[73] Z. Wang,[14] Z. Wang,[4,p] Z. Wang,[30] J. A. Ward,[57,1] M. Waterlaat,[49] N. K. Watson,[54] D. Websdale,[62] Y. Wei,[6] J. Wendel,[81] B. D. C. Westhenry,[55] C. White,[56] M. Whitehead,[60] E. Whiter,[54] A. R. Wiederhold,[63] D. Wiedner,[19] G. Wilkinson,[64] M. K. Wilkinson,[66] M. Williams,[65] M. J. Williams,[49] M. R. J. Williams,[59] R. Williams,[56] Z. Williams,[55] F. F. Wilson,[58] M. Winn,[12] W. Wislicki,[42] M. Witek,[41] L. Witola,[22] G. Wormser,[14] S. A. Wotton,[56] H. Wu,[69] J. Wu,[8] X. Wu,[74] Y. Wu,[6] Z. Wu,[7] K. Wyllie,[49] S. Xian,[72] Z. Xiang,[5] Y. Xie,[8] A. Xu,[35] J. Xu,[7] L. Xu,[4,p] L. Xu,[4,p] M. Xu,[57] Z. Xu,[49] Z. Xu,[7] Z. Xu,[5] K. Yang,[62] S. Yang,[7] X. Yang,[6] Y. Yang,[29,j] Z. Yang,[6] V. Yeroshenko,[14] H. Yeung,[63] H. Yin,[8] X. Yin,[7] C. Y. Yu,[6] J. Yu,[71] X. Yuan,[5] Y Yuan,[5,7] E. Zaffaroni,[50] M. Zavertyaev,[21] M. Zdybal,[41] F. Zenesini,[25,i] C. Zeng,[5,7] M. Zeng,[4,p] C. Zhang,[6] D. Zhang,[8] J. Zhang,[7] L. Zhang,[4,p] S. Zhang,[71] S. Zhang,[64] Y. Zhang,[6] Y. Z. Zhang,[4,p] Y. Zhao,[22] A. Zharkova,[44] A. Zhelezov,[22] S. Z. Zheng,[6] X. Z. Zheng,[4,p] Y. Zheng,[7] T. Zhou,[6] X. Zhou,[8] Y. Zhou,[7] V. Zhovkovska,[57] L. Z. Zhu,[7] X. Zhu,[4,p] X. Zhu,[8] V. Zhukov,[17] J. Zhuo,[48] Q. Zou,[5,7] D. Zuliani,[33,g] and G. Zunica[50]

(LHCb Collaboration)

[1]*School of Physics and Astronomy, Monash University, Melbourne, Australia*
[2]*Centro Brasileiro de Pesquisas Físicas (CBPF), Rio de Janeiro, Brazil*
[3]*Universidade Federal do Rio de Janeiro (UFRJ), Rio de Janeiro, Brazil*
[4]*Department of Engineering Physics, Tsinghua University, Beijing, China*
[5]*Institute of High Energy Physics (IHEP), Beijing, China*
[6]*School of Physics State Key Laboratory of Nuclear Physics and Technology, Peking University, Beijing, China*
[7]*University of Chinese Academy of Sciences, Beijing, China*
[8]*Institute of Particle Physics, Central China Normal University, Wuhan, Hubei, China*
[9]*Consejo Nacional de Rectores (CONARE), San Jose, Costa Rica*
[10]*Université Savoie Mont Blanc, CNRS, IN2P3-LAPP, Annecy, France*
[11]*Université Clermont Auvergne, CNRS/IN2P3, LPC, Clermont-Ferrand, France*
[12]*Université Paris-Saclay, Centre d'Etudes de Saclay (CEA), IRFU, Saclay, France, Gif-Sur-Yvette, France*
[13]*Aix Marseille Université, CNRS/IN2P3, CPPM, Marseille, France*
[14]*Université Paris-Saclay, CNRS/IN2P3, IJCLab, Orsay, France*
[15]*Laboratoire Leprince-Ringuet, CNRS/IN2P3, Ecole Polytechnique, Institut Polytechnique de Paris, Palaiseau, France*
[16]*LPNHE, Sorbonne Université, Paris Diderot Sorbonne Paris Cité, CNRS/IN2P3, Paris, France*
[17]*I. Physikalisches Institut, RWTH Aachen University, Aachen, Germany*
[18]*Universität Bonn—Helmholtz-Institut für Strahlen und Kernphysik, Bonn, Germany*
[19]*Fakultät Physik, Technische Universität Dortmund, Dortmund, Germany*
[20]*Physikalisches Institut, Albert-Ludwigs-Universität Freiburg, Freiburg, Germany*
[21]*Max-Planck-Institut für Kernphysik (MPIK), Heidelberg, Germany*

[22]Physikalisches Institut, Ruprecht-Karls-Universität Heidelberg, Heidelberg, Germany
[23]School of Physics, University College Dublin, Dublin, Ireland
[24]INFN Sezione di Bari, Bari, Italy
[25]INFN Sezione di Bologna, Bologna, Italy
[26]INFN Sezione di Ferrara, Ferrara, Italy
[27]INFN Sezione di Firenze, Firenze, Italy
[28]INFN Laboratori Nazionali di Frascati, Frascati, Italy
[29]INFN Sezione di Genova, Genova, Italy
[30]INFN Sezione di Milano, Milano, Italy
[31]INFN Sezione di Milano-Bicocca, Milano, Italy
[32]INFN Sezione di Cagliari, Monserrato, Italy
[33]INFN Sezione di Padova, Padova, Italy
[34]INFN Sezione di Perugia, Perugia, Italy
[35]INFN Sezione di Pisa, Pisa, Italy
[36]INFN Sezione di Roma La Sapienza, Roma, Italy
[37]INFN Sezione di Roma Tor Vergata, Roma, Italy
[38]Nikhef National Institute for Subatomic Physics, Amsterdam, Netherlands
[39]Nikhef National Institute for Subatomic Physics and VU University Amsterdam, Amsterdam, Netherlands
[40]AGH—University of Krakow, Faculty of Physics and Applied Computer Science, Kraków, Poland
[41]Henryk Niewodniczanski Institute of Nuclear Physics Polish Academy of Sciences, Kraków, Poland
[42]National Center for Nuclear Research (NCBJ), Warsaw, Poland
[43]Horia Hulubei National Institute of Physics and Nuclear Engineering, Bucharest-Magurele, Romania
[44]Authors affiliated with an institute formerly covered by a cooperation agreement with CERN
[45]DS4DS, La Salle, Universitat Ramon Llull, Barcelona, Spain
[46]ICCUB, Universitat de Barcelona, Barcelona, Spain
[47]Instituto Galego de Física de Altas Enerxías (IGFAE), Universidade de Santiago de Compostela, Santiago de Compostela, Spain
[48]Instituto de Fisica Corpuscular, Centro Mixto Universidad de Valencia—CSIC, Valencia, Spain
[49]European Organization for Nuclear Research (CERN), Geneva, Switzerland
[50]Institute of Physics, Ecole Polytechnique Fédérale de Lausanne (EPFL), Lausanne, Switzerland
[51]Physik-Institut, Universität Zürich, Zürich, Switzerland
[52]NSC Kharkiv Institute of Physics and Technology (NSC KIPT), Kharkiv, Ukraine
[53]Institute for Nuclear Research of the National Academy of Sciences (KINR), Kyiv, Ukraine
[54]School of Physics and Astronomy, University of Birmingham, Birmingham, United Kingdom
[55]H.H. Wills Physics Laboratory, University of Bristol, Bristol, United Kingdom
[56]Cavendish Laboratory, University of Cambridge, Cambridge, United Kingdom
[57]Department of Physics, University of Warwick, Coventry, United Kingdom
[58]STFC Rutherford Appleton Laboratory, Didcot, United Kingdom
[59]School of Physics and Astronomy, University of Edinburgh, Edinburgh, United Kingdom
[60]School of Physics and Astronomy, University of Glasgow, Glasgow, United Kingdom
[61]Oliver Lodge Laboratory, University of Liverpool, Liverpool, United Kingdom
[62]Imperial College London, London, United Kingdom
[63]Department of Physics and Astronomy, University of Manchester, Manchester, United Kingdom
[64]Department of Physics, University of Oxford, Oxford, United Kingdom
[65]Massachusetts Institute of Technology, Cambridge, Massachusetts, USA
[66]University of Cincinnati, Cincinnati, Ohio, USA
[67]University of Maryland, College Park, Maryland, USA
[68]Los Alamos National Laboratory (LANL), Los Alamos, New Mexico, USA
[69]Syracuse University, Syracuse, New York, USA
[70]Pontifícia Universidade Católica do Rio de Janeiro (PUC-Rio), Rio de Janeiro, Brazil
(associated with Universidade Federal do Rio de Janeiro (UFRJ),
Rio de Janeiro, Brazil)
[71]School of Physics and Electronics, Hunan University, Changsha City, China
(associated with Institute of Particle Physics, Central China Normal University,
Wuhan, Hubei, China)
[72]Guangdong Provincial Key Laboratory of Nuclear Science, Guangdong-Hong Kong Joint Laboratory of Quantum Matter,
Institute of Quantum Matter, South China Normal University, Guangzhou, China
(associated with Department of Engineering Physics, Tsinghua University, Beijing, China)
[73]Lanzhou University, Lanzhou, China
(associated with Institute of High Energy Physics (IHEP), Beijing, China)

[74]School of Physics and Technology, Wuhan University, Wuhan, China
(associated with Department of Engineering Physics, Tsinghua University, Beijing, China)
[75]Departamento de Fisica, Universidad Nacional de Colombia, Bogota, Colombia
(associated with LPNHE, Sorbonne Université, Paris Diderot Sorbonne Paris Cité, CNRS/IN2P3, Paris, France)
[76]Ruhr Universitaet Bochum, Fakultaet für Physik und Astronomie, Bochum, Germany
(associated with Fakultät Physik, Technische Universität Dortmund,
Dortmund, Germany)
[77]Eotvos Lorand University, Budapest, Hungary
(associated with European Organization for Nuclear Research (CERN), Geneva, Switzerland)
[78]Van Swinderen Institute, University of Groningen, Groningen, Netherlands
(associated with Nikhef National Institute for Subatomic Physics,
Amsterdam, Netherlands)
[79]Universiteit Maastricht, Maastricht, Netherlands
(associated with Nikhef National Institute for Subatomic Physics, Amsterdam, Netherlands)
[80]Tadeusz Kosciuszko Cracow University of Technology, Cracow, Poland
(associated with Henryk Niewodniczanski Institute of Nuclear Physics Polish Academy of Sciences,
Kraków, Poland)
[81]Universidade da Coruña, A Coruña, Spain
(associated with DS4DS, La Salle, Universitat Ramon Llull, Barcelona, Spain)
[82]Department of Physics and Astronomy, Uppsala University, Uppsala, Sweden
(associated with School of Physics and Astronomy, University of Glasgow,
Glasgow, United Kingdom)
[83]University of Michigan, Ann Arbor, Michigan, USA
(associated with Syracuse University, Syracuse, New York, USA)

[a]Deceased.
[b]Also at Lamarr Institute for Machine Learning and Artificial Intelligence, Dortmund, Germany.
[c]Also at Università degli Studi di Milano-Bicocca, Milano, Italy.
[d]Also at Università di Roma Tor Vergata, Roma, Italy.
[e]Also at Scuola Normale Superiore, Pisa, Italy.
[f]Also at Università di Ferrara, Ferrara, Italy.
[g]Also at Università di Padova, Padova, Italy.
[h]Also at Facultad de Ciencias Fisicas, Madrid, Spain.
[i]Also at Università di Bologna, Bologna, Italy.
[j]Also at Università di Genova, Genova, Italy.
[k]Also at Università degli Studi di Milano, Milano, Italy.
[l]Also at Universidad Nacional Autónoma de Honduras, Tegucigalpa, Honduras.
[m]Also at Università di Cagliari, Cagliari, Italy.
[n]Also at Centro Federal de Educacão Tecnológica Celso Suckow da Fonseca, Rio De Janeiro, Brazil.
[o]Also at Università di Bari, Bari, Italy.
[p]Also at Center for High Energy Physics, Tsinghua University, Beijing, China.
[q]Also at Università di Perugia, Perugia, Italy.
[r]Also at LIP6, Sorbonne Université, Paris, France.
[s]Also at Università di Pisa, Pisa, Italy.
[t]Also at Hangzhou Institute for Advanced Study, UCAS, Hangzhou, China.
[u]Also at School of Physics and Electronics, Henan University, Kaifeng, China.
[v]Also at Università di Bergamo, Bergamo, Italy.
[w]Also at Università di Siena, Siena, Italy.
[x]Also at Department of Physics/Division of Particle Physics, Lund, Sweden.
[y]Also at Università della Basilicata, Potenza, Italy.
[z]Also at Universidad de Alcalá, Alcalá de Henares, Spain.
[aa]Also at Università di Urbino, Urbino, Italy.